A Case Study for Marine Low-Head Pumped Hydro Storage in the Caribbean Region of Colombia

J.P. Hoffstaedt[1], A. Jarquin-Laguna[1], D.P.K. Truijen[2], J.D.M. De Kooning[2], K. Stockman[2]

1. Faculty of Mechanical, Maritime and Materials Engineering, Department of Maritime and Transport Technology, Delft University of Technology, Mekelweg 2, 2628 CD Delft, the Netherlands
2. Department of Electromechanical Systems & Metal Engineering, Ghent University & FlandersMake@UGent - Corelab MIRO, Sint-Martens-Latemlaan 2B, 8500 Kortrijk, Belgium

Keywords— **Energy Transition, Grid Stability, Low-Head Pumped Hydro Storage, Numerical Modelling, Reversible Pump-Turbine**

I. INTRODUCTION

Rapidly rising shares of renewable energy sources in electricity grids around the world could cause a potential threat to the stability and quality of our power supply. To balance out the mismatch between an intermittent supply and fluctuating demand the deployment of large scale energy storage is required [1]. Moreover, the concurrent reduction of spinning reserves is predicted to likely raise the demand for the provision of ancillary services [2]. To tackle both of these challenges, a novel low-head pumped storage system (LH-PHS) is proposed. Shifting the operating range from traditional high head applications to low and ultra-low heads could allow the deployment of pumped storage technology in regions where so far deemed not feasible [3]. Aimed at coastal areas and shallow seas, the system offers the potential for deployment alongside offshore renewable generators, creating in combination, a dispatchable energy source. A full scale system would consist of a ring dam and several reversible pump-turbine units enabling further spatial and economic synergies with offshore generators. These synergies may include shared interconnectors, civil structures or the deployment of wind turbines or wave energy generators within or adjacent to the dam.

To evaluate the potential of the proposed low-head pumped storage plant to contribute to grid stability, a case study is performed. The system is applied to the Caribbean region of Colombia in sea depths of up to 21 m. In a first step a quasi-static model is used to simulate a full balancing cycle including pump and turbine mode of that storage plant. To further look into the systems capability to provide ancillary services, a parametric analysis is conducted investigating the influence of different system components on the time response of the power output. For this, a system model covering relevant dynamics is used.

II. METHODOLOGY

A schematic of the proposed LH-PHS plant is shown in Fig. 1. The upper reservoir shown on the left of the dam is the sea and the lower reservoir is encapsulated by the dam. The newly designed reversible pump-turbine (RPT) consists of two contra-rotating runners, each of which is connected to a permanent magnet synchronous motor-generator. These are connected to the grid via an AC-DC-AC coupling. Each RPT set has a design power capacity of 10MW and a diameter of 6 meter. The deployed system will use a ring dam and a series of powerhouses adjacent to each other allowing to scale the systems power capacity in 10MW increments. The system can be operated in variable speed, with each runner being controlled individually.

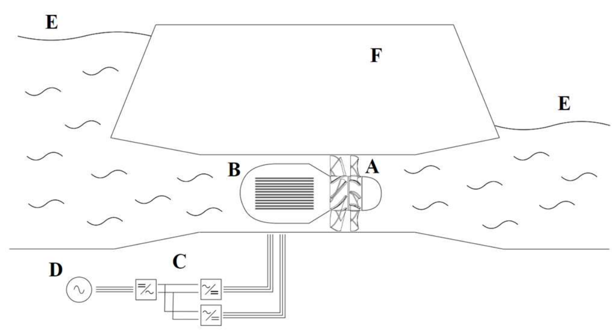

Fig. 1. Schematic of the proposed low-head pumped storage plant in cross-sectional view including: **A** Contra-Rotating Runners, **B** Axial-Flux Motor-generators, **C** AC-DC-AC Coupling, **D** Grid, **E** Upper/Lower Reservoir, **F** Dam [4]

The offshore wind roadmap of Colombia has estimated the potential of offshore wind deployment at 50 GW considering environmental, social and technical constraints [5]. To balance out the intermittency and reduction in spinning reserves this will introduce into the power grid, large scale storage capable of delivering ancillary services such as frequency regulation is required. Deploying the proposed system in the coastal areas and shallow seas of the Caribbean region of Colombia carries significant potential to aid grid stability.

For this, the system is scaled to a total power capacity of 1 GW. The net energy capacity in generation mode is set to 4GWh leading to a total reservoir area of 47.5 km^2. A detailed site assessment is not within the scope of this study, however, the system could be ideally deployed near the coast with a sea depth of between 16 m and 21 m. A sea depth below 21 m, considering the inlet diameter, minimum submergence and max head range, would require the RPTs to be partially submerged into the seabed.

A. *Quasi-static model*

To model the operation of the plant over a full balancing cycle in turbine and pump mode, a quasi-static model is used. At the core of the model is the characterisation of the RPT. This characterisation is based on a range of steady-state CFD simulations as per Fahlbeck et al. [6]. From this characterisation, maximum efficiency maps are created determining the best operating point for any given head difference over the RPT and desired power setpoint.

The operating points can be reached utilising three degrees of freedom in the control. These are the two angular velocities of the RPT and a valve. Combined with the major and minor hydraulic losses as well as the power take-off losses, the flow and power output/input can be obtained. This method as well as all relevant system parameters are described in detail by Truijen et al. [7].

B. *Dynamic system model*

In order to model the dynamic behaviour of the plant a system model is developed incorporating the conduit, RPT and drivetrain. The conduit is modelled using a 1-D approach considering compressibility effects and including both steady and unsteady friction. The equations are solved using a central-schemed finite difference method and the boundaries are developed using characteristic equations. Both drivetrains are modelled individually assuming a rigid shaft, lumping together the inertia of the RPT, driveshaft and rotational component of the motor-generators. The conduit and drivetrain models are coupled via the RPT characterisation, where the head over each runner and their respective efficiency is obtained as a function of their tip speed ratios. A detailed description of the system model is given by Hoffstaedt et al. [8].

III. RESULTS

C. *Energy balancing*

The operational limits of the plant are set from 1 MW to 10 MW per RPT (100 MW to 1 GW for the full plant) in both pump and turbine mode. This leads to a gross head range of between 3.05 m and 9 m. Below the lower limit 1 MW cannot be achieved in turbine mode and above 9 m 10 MW is exceeded in pump mode. The control strategy of the plant is based on tracking the maximum efficiency point for any given head difference between the reservoirs. In turbine mode this also correlates with the maximum power setpoints. In the model, the water level of the upper reservoir is set to a constant 9 m. Since the tidal range in the Caribbean region is very small, all tidal changes are neglected in this study. Fig. 2 shows the change of water elevation of the lower reservoir over the full balancing cycle. It should be noted that a head of 0 m does not represent a fully empty reservoir but rather the minimum water level since the inlet to the RPTs needs to always be submerged by 2 m.

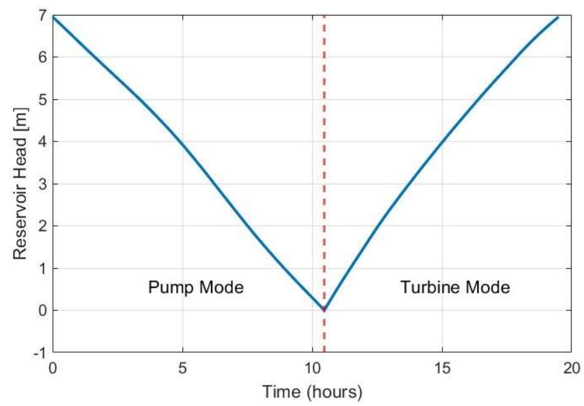

Fig. 2. Head of the lower reservoir over a full balancing cycle

In pump mode it takes 10 hours and 28 minutes to fully empty the reservoir from the initial maximum head of 6.95 m. In turbine mode the reservoir is filled again within 9 hours and 2 minutes. The flow rate and power during the cycle are shown in Fig. 3 and Fig. 4 respectively. The flow rate is given per RPT unit and the power output is given for the full plant.

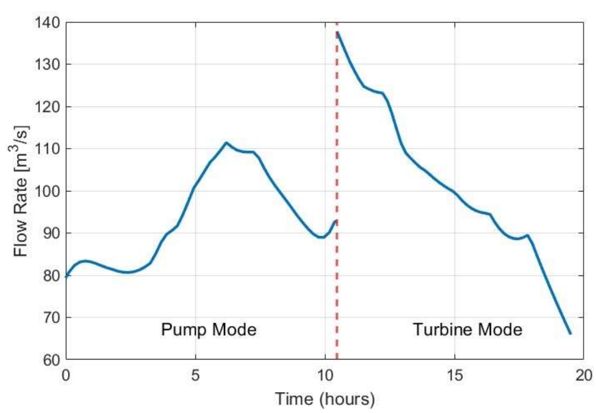

Fig. 3. Flow rate of each RPT unit during turbine and pump mode

Additionally to the 1 to 10 MW range defined for each RPT, there are limits to the maximum torque of each runner. Further limiting the maximum power output are the hydraulic losses at very high flow rates. In combination this leads to a maximum achievable power for each head difference. In turbine mode a more linear trend for both power and flow rate can be observed. This is due to the fact that the maximum efficiency correlates with this maximum power under the constraints described above. The other fluctuations are caused by changes in efficiency

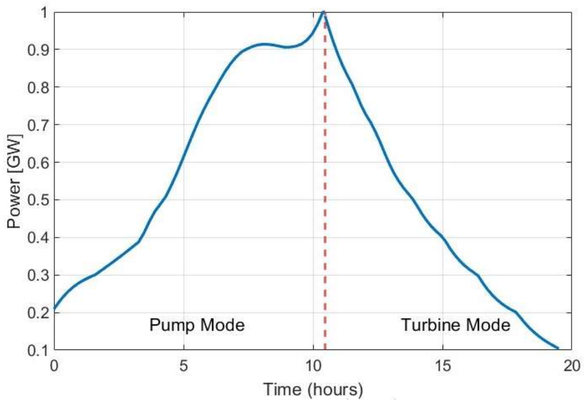

Fig. 4. Total power of the plant over the balancing cycle

across the operating range. The total system efficiency is shown in Fig. 5. This includes both runners of the RPTs combined as well as all hydraulic, drivetrain and motor-generator losses. The main factors that influence that efficiency over the operating range are flow rate, angular velocity of the runners and most importantly the RPT efficiency at different operating points.

This is most notable towards the beginning of pump mode and the end of turbine mode. Here the head difference is below 4 m and the efficiency of the RPT drops

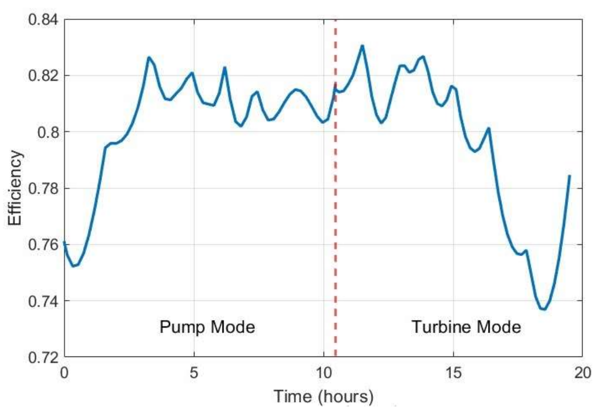

Fig. 5. Full system efficiency including both runners, hydraulic, drivetrain and motor-generator losses across the balancing cycle

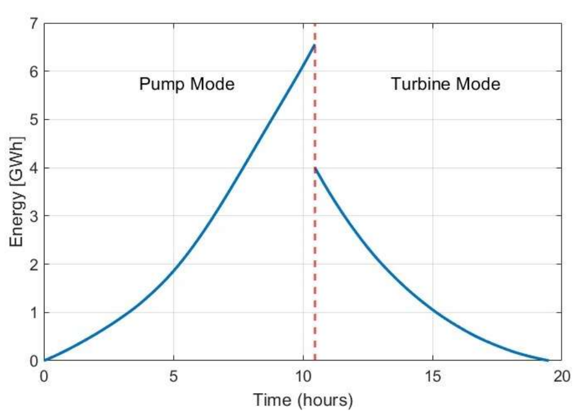

Fig. 6. Total Energy stored and recouped during the balancing cycle – For each mode this reflects the net energy input/output into the plant

rapidly. Considering the full system efficiency the total energy input and output of the plant is shown in Fig. 6. The depicted values represent the net energy input to the plant in pump mode and the net energy output in turbine mode. During the pump cycle a total of 6.56 GWh are put in and a total of 4 GWh are recouped in turbine mode. This leads to an overall roundtrip efficiency of ~61 %.

D. Dynamic response simulation

To evaluate the dynamic response of the system and what parameters influence it, dynamic simulations are carried out varying the inertia of the conduit and both drivetrains. The system is initially operating in steady state with a gross head of 9 m in turbine mode and a power output of 5.25 MW per RPT. After 50 seconds, a torque step is injected for both runners reducing the generator torque from 0.97 MNm for runner 1 and 1.37 MNm for runner 2 by 6.5 %. The resulting new operating point increases the power to 9.8 MW.

The first simulation based on this torque step assumes a conduit length of 60 m and runners made from stainless steel. The second case changes the runner material to aluminium with no changes to the remaining drivetrains. This results in a decrease in rotational inertia of 52 % for the first drivetrain and 56% for the second drivetrain. For the third case, stainless steel runners are used and the conduit length is doubled to 120. The resulting change in power output for all three cases is shown in Fig. 7.

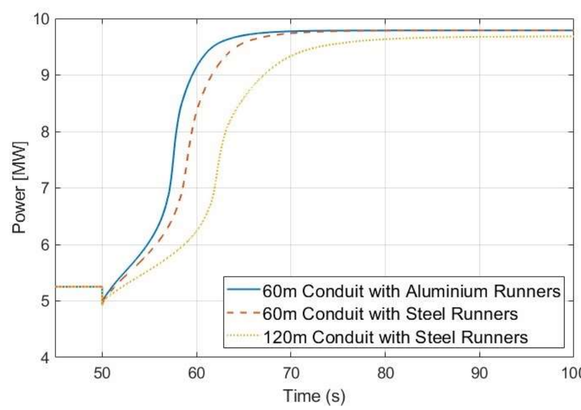

Fig. 7. Response of power output for varying conduit and drivetrain inertia

As expected the fastest response is obtained with the short conduit and aluminium runners. It can also be observed that the inertia of the water column has a significantly larger effect on the response time compared to a reduction in rotational inertia in the drivetrains. The change in flow rate and the angular velocity of runner 1 is shown in Fig. 8 and Fig. 9. The response of runner 2 shows very similar trends and is therefore not depicted separately.

The small horizontal section visible in the flow rates corresponds to a rapid improvement in efficiency as the tip speed ratio of both runners increases. The simulation using the 120 m conduit results in a slightly lower steady state

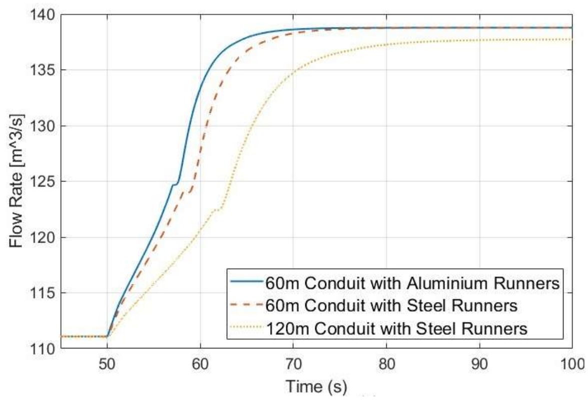

Fig. 8. Response of flow rate for varying conduit and drivetrain inertia

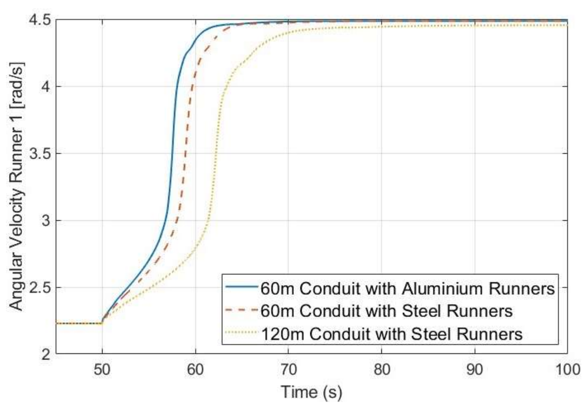

Fig. 9. Response of the angular velocity of runner 1 for varying conduit and drivetrain inertia

value for the flow rate, angular velocities and power output due to the increased hydraulic losses. The effect on the dynamic response however is negligible. It should also be noted that since the conduit and both runners of the RPT are directly coupled, the individual response of the flow rate and angular velocities do not reflect the individual changes to conduit and drivetrain inertias.

To counteract the potential decrease in grid stability caused by rising shares of inverter-coupled renewable generators, one of the major ancillary services required is frequency control. Aside from grid inertia, primary frequency control provides a fast response to deviations in nominal grid frequency. Power plants are required to provide this primary response within 30 s [9] with it being proposed that non-synchronous plants need to be able to adjust their power by 2 – 6 % within 15 s [10]. The dynamic response of the proposed storage plant in all configurations reaches a power increase of around 85 % in 20 – 30 s. Applying a control algorithm to the system will likely improve this response time further.

IV. CONCLUSION

The presented study has shown the technical viability of utilising the proposed low-head pumped storage system to improve grid stability under a rapid increase in the penetration of renewable generators into our grids. It can balance out the mismatch between an intermittent supply and a fluctuating demand with a roundtrip efficiency of around 61 % including all hydraulic and power take-off losses. It can be operated under a wide variety of operating conditions and desired power outputs. The dynamic simulations have shown that it is also capable of rapidly ramping up power enabling it to provide crucial ancillary services.

One of the major disadvantages of the proposed system is the large footprint. Further studies may investigate the effect of increasing the power and torque rating of the motor-generators allowing for a larger head range and therefore reduced reservoir size. Additionally, a detailed economic analysis of the proposed system based on this technical case study could further evaluate the viability of the proposed solution.

ACKNOWLEDGEMENTS

This research is part of a project that has received funding from the European Union's Horizon 2020 research and innovation programme under grant agreement No. 883553.

REFERENCES

[1] Q. Gao, R. Yuan, N. Ertugrul, B. Ding, J. A. Hayward, and Y. Li, “Analysis of energy variability and costs for offshore wind and hybrid power unit with equivalent energy storage system,” *Applied Energy*, 2023, doi: 10.1016/j.apenergy.2023.121192.

[2] M. G. Pollitt and K. L. Anaya, “Competition in Markets for Ancillary Services? The Implications of Rising Distributed Generation,” *Energy J.*, vol. 41, pp. 5–31, 2020, doi: 10.5547/01956574.41.SI1.MPOL.

[3] J.P. Hoffstaedt, D.P.K. Truijen, J. Fahlbeck, L.H.A. Gans, M. Qudaih, A.J. Laguna, J.D.M. De Kooning, K. Stockman, H. Nilsson, P.-T. Storli, B. Engel, M. Marence, J.D. Bricker,”Low-head pumped hydro storage: A review of applicable technologies for design, grid integration, control and modelling,” *Renewable and Sustainable Energy Reviews*, vol. 158, 2022, https://doi.org/10.1016/j.rser.2022.112119.

[4] J. P. Hoffstaedt, R. Ansorena Ruiz, D. Schuerenkamp, A. Jarquin-Laguna, and N. Goseberg, “Experimental setup and methods for a novel low-head pumped storage system,” in *IET OSES2023 Event Proceedings*, 2023

[5] The Renewables Consulting Group, “Offshore wind roadmap for Colombia,” [Online]. Available: https://www.minenergia.gov.co/documents/5859/Colombia_Offshore_Wind_Roadmap_VE_compressed.pdf

[6] J. Fahlbeck, H. Nilsson, S. Salehi, M. Zangeneh, and M. Joseph, “Numerical analysis of an initial design of a counter-rotating pump-turbine," in *IOP Conference Series Earth and Environmental Science*, 2021

[7] D. P. K. Truijen, J.P. Hoffstaedt , J. D. M. De Kooning, A. Jarquin-Laguna , J.Fahlbeck , H. Nilsson, and Kurt Stockman, “Improving Low-Head Pumped Hydropower Storage Efficiency: The Impact of Speed Ratio and Inlet Valve Control on Contra-Rotating Pump-Turbines,” [to be published]

[8] J.P. Hoffstaedt, A. Jarquin-Laguna, J. Fahlbeck, and H. Nilsson, “System model development and numerical simulation of low-head pumped hydro storage,” in *Trends in Renewable Energies Offshore*, 2022

[9] S.X. Carvajal, J. Serrano, S. Arango, “Colombian ancillary services and international connections: Current weaknesses and

policy challenges," *Energy Policy*, vol. 52, 2013, https://doi.org/10.1016/j.enpol.2012.10.041.

[10] Gerencia Centro Nacional de Despacho, "Propuesta de requerimientos tecnicos para la integracion de fuentes de generacion no sincrona al sin," 2017